PHYSICAL REVIEW A **76**, 032507 (2007)

Improved dipole moments by combining short-range gradient-corrected density-functional theory with long-range wave-function methods

Erich Goll and Hermann Stoll[*]
Institut für Theoretische Chemie, Universität Stuttgart, D-70550 Stuttgart, Germany

Christian Thierfelder and Peter Schwerdtfeger[†]
Centre of Theoretical Chemistry and Physics, The Institute of Advanced Studies and the Institute of Fundamental Sciences, Massey University (Albany Campus), Private Bag 102904, North Shore MSC, Auckland, New Zealand

(Received 14 May 2007; published 20 September 2007)

Previously proposed schemes of coupling short-range density-functional-based with long-range wave-function-based methods are tested for the notoriously difficult case of correctly describing the charge distribution in compounds containing late transition elements. We show that for the dipole moments of the group-11 transition metal hydrides and halides the recently developed Coulomb-attenuated Becke three-parameter Lee-Yang-Parr hybrid functional already leads to a substantial improvement compared to other density functionals. Further improvement is achieved by combining a gradient-corrected short-range functional of the Perdew-Burke-Ernzerhof type with coupled-cluster theory. The results clearly demonstrate that mixing of long-range *ab initio* Hartree-Fock and post-Hartree-Fock methods helps to remove deficiencies of current density functionals.

DOI: 10.1103/PhysRevA.76.032507 PACS number(s): 31.15.Ar, 31.15.Dv, 31.15.Ew, 33.15.Kr

I. INTRODUCTION

Density-functional theory (DFT) and wave-function-based *ab initio* methods are to some extent complementary. DFT provides a very efficient (and yet reliable) treatment of dynamical correlation effects, in a formally independent-particle framework with modest basis sets, while an accurate *ab initio* description is computer time expensive. On the other hand, *ab initio* methods provide an efficient treatment of static correlation and near degeneracies and also of long-range correlation, where DFT approximations currently are less reliable.

Let us mention some shortcomings in approximating (formally exact) DFT. For example the local-density approximation (LDA) and the generalized-gradient approximations (GGA) are local or semilocal and do not include highly nonlocal long-range dispersive-type (van der Waals) interactions [1]. As a result, most GGAs do not lead to binding for rare gas dimers in the gas phase [2]. Second, strongly correlated systems like Mott insulators of transition metal compounds are not well described by GGAs [3], and consequently an on-site repulsion Hubbard-like term is commonly added (LDA+U approach [4]) to improve the description of electron correlation in d shells. In fact, transition-metal- or f-element-containing compounds are a problematic class of materials for DFT, as the charge distribution in these compounds is not well described by either the LDA or variants of the GGA [5,6]. Spin symmetry breaking in transition metal compounds and consequently spin-spin coupling in magnetic materials are also affected by these deficiencies [7,8].

On the other hand, one of the shortcomings in wave-function-based theories is the need for extensive basis sets and rather long configuration expansions due to the difficulty of explicitly describing the interelectronic cusp of the wave function. It has therefore been suggested [9–12] to relieve wave-function-based methods from the description of this cusp, by splitting off the short-range (SR) part, containing the singularity at $r_{ij}=0$, from the interelectronic interaction operator $\Sigma_{i<j}1/r_{ij}$ of the Hamiltonian. The SR (exchange-)correlation contributions are then calculated by DFT, and *ab initio* methods are applied to the smooth long-range (LR) part only.

In this paper, we use such a coupling in order to remove some of the DFT deficiencies mentioned above. An ideal test ground is the group-11 halides where the performance of DFT is less than satisfactory. It was shown only recently that dipole moments of transition metal compounds are not well described by standard or hybrid GGAs [5,13]. Dipole moments are underestimated in some cases by more than 0.5 D for the group-11 halides at the Becke three-parameter Lee-Yang-Parr (B3LYP) [14] level of theory [13]. This rather poor description of the valence charge density in turn results in a poor description of the charge density distribution close to the nucleus. Thus electric field gradients at the nucleus are affected as well, leading to completely unreliable results [5,15]. First, we apply the Coulomb-attenuated (CAM) B3LYP functional, a functional recently developed by Yanai, Tew, and Handy [16], within an all-electron Dirac-Coulomb formalism. This functional already gave notably improved properties like dipole polarizabilities compared to the standard B3LYP functional [17]. We then check whether a combination of SR LDA and SR GGA functionals with LR Møller-Plesset second-order perturbation (MP2) theory and with LR coupled-cluster (CC) methods—namely, LR CC with single and double excitations (LR CCSD) and with additional perturbative triples [LR CCSD(T)] [18,19]—can further improve the situation. For these purposes we used the already existing SR LDA functionals [20,21] as well as our lately developed SR GGA functional [22,23] of the Perdew-Burke-Ernzerhof (PBE) type [24].

---

[*] stoll@theochem.uni-stuttgart.de

[†] p.a.schwerdtfeger@massey.ac.nz

II. METHODS

The above-mentioned short-range–long-range decomposition of the interelectronic interaction operator of the Hamiltonian is done using the standard error function erf and its complement erfc=1−erf:

$$V_{ee} = \underbrace{\sum_{i<j} \frac{\operatorname{erfc}(\mu r_{ij})}{r_{ij}}}_{V_{ee}^{\mathrm{SR}}} + \underbrace{\sum_{i<j} \frac{\operatorname{erf}(\mu r_{ij})}{r_{ij}}}_{V_{ee}^{\mathrm{LR}}}. \tag{1}$$

Then the appropriate short-range density functional can be constructed using Levy's constrained-search formalism [25]. We start with the standard formula for the ground-state energy:

$$E_0 = \min_{\rho}(\min_{\Psi\to\rho}\langle\Psi|T + V_{ne} + V_{ee}|\Psi\rangle). \tag{2}$$

Subtracting and adding $\langle\Psi|T+V_{ne}+V_{ee}^{\mathrm{LR}}|\Psi\rangle$, i.e., the expression to be treated explicitly by wave-function methods, yields

$$E_0 = \min_{\rho}(\min_{\Psi\to\rho}\langle\Psi|T + V_{ne} + V_{ee}|\Psi\rangle - \min_{\Psi\to\rho}\langle\Psi|T + V_{ne} + V_{ee}^{\mathrm{LR}}|\Psi\rangle + \min_{\Psi\to\rho}\langle\Psi|T + V_{ne} + V_{ee}^{\mathrm{LR}}|\Psi\rangle). \tag{3}$$

Canceling out $\langle\Psi|V_{ne}|\Psi\rangle$ in the first two terms on the right-hand side leads to

$$E_0 = \min_{\rho}(E_0^{\mathrm{SR}}[\rho] + \min_{\Psi\to\rho}\langle\Psi|T + V_{ne} + V_{ee}^{\mathrm{LR}}|\Psi\rangle), \tag{4}$$

$$E_0^{\mathrm{SR}}[\rho] = \min_{\Psi\to\rho}\langle\Psi|T + V_{ee}|\Psi\rangle - \min_{\Psi\to\rho}\langle\Psi|T + V_{ee}^{\mathrm{LR}}|\Psi\rangle, \tag{5}$$

where E_0^{SR} constitutes a (universal) short-range energy functional E_0^{SR}, which, in turn, can be split into a Hartree term J^{SR} and an exchange-correlation term $E_{\mathrm{xc}}^{\mathrm{SR}}$:

$$E_0^{\mathrm{SR}}[\rho] = J^{\mathrm{SR}}[\rho] + E_{\mathrm{xc}}^{\mathrm{SR}}[\rho], \tag{6}$$

$$J^{\mathrm{SR}}[\rho] = \frac{1}{2}\int \rho(r_1)\frac{\operatorname{erfc}(\mu r_{12})}{r_{12}}\rho(r_2)dr_1 dr_2. \tag{7}$$

Equations (5)–(7) define the short-range exchange-correlation density functional $E_{\mathrm{xc}}^{\mathrm{SR}}$, which contains the difference of exchange-correlation between full and long-range interaction, as well as corresponding kinetic-energy contributions. We point out that this procedure is very similar to that used in standard density-functional theory. So far, everything is exact. $E_{\mathrm{xc}}^{\mathrm{SR}}$ can be approximated in different ways. In this paper we use specially designed short-range functionals of the LDA [20,21] and GGA [22,23] type. Note that the value of the parameter κ, occurring in the definition of the GGA exchange functional [22,23], should be corrected to 0.804.

As an immediate consequence of Eqs. (4) and (6), we have

$$E_0 = \min_{\Psi}\{\langle\Psi|T + V_{ne} + V_{ee}^{\mathrm{LR}}|\Psi\rangle + J^{\mathrm{SR}}[\rho_\Psi] + E_{\mathrm{xc}}^{\mathrm{SR}}[\rho_\Psi]\}. \tag{8}$$

Here, ρ_Ψ is the one-particle density associated with Ψ. It is easy to show by variation of Ψ that the "long-range" wave function Ψ^{LR} minimizing the expression within the curly brackets on the right-hand side of Eq. (8) must be an eigenfunction of the Hamiltonian

$$\hat{H}_{\mathrm{SR-KS}}^{\mathrm{LR}} = T + V_{ne} + V_{ee}^{\mathrm{LR}} + V_H^{\mathrm{SR}}[\rho] + V_{\mathrm{xc}}^{\mathrm{SR}}[\rho], \tag{9}$$

where $V_H^{\mathrm{SR}} = \frac{\delta J^{\mathrm{SR}}}{\delta\rho}$ (i.e., the short-range Hartree potential) and $V_{\mathrm{xc}}^{\mathrm{SR}} = \frac{\delta E_{\mathrm{xc}}^{\mathrm{SR}}}{\delta\rho}$ (i.e., the short-range exchange-correlation potential) are density-dependent one-electron potentials supplementing the long-range Hamiltonian $T+V_{ne}+V_{ee}^{\mathrm{LR}}$. This means that standard *ab initio* methods of quantum chemistry can be applied to the problem at hand, with three modifications: (a) All two-electron integrals must be calculated with the long-range interelectronic interaction V_{ee}^{LR}, instead of the full interaction V_{ee}; (b) additional one-electron potentials $(V_H^{\mathrm{SR}}[\rho]+V_{\mathrm{xc}}^{\mathrm{SR}}[\rho])$ have to be included when calculating Ψ^{LR}; (c) the ground-state energy E_0 must be calculated from Eq. (8) rather than from the expectation value of $\hat{H}_{\mathrm{SR-KS}}^{\mathrm{LR}}$. Note that $\hat{H}_{\mathrm{SR-KS}}^{\mathrm{LR}}$ approaches the usual Kohn-Sham operator of DFT, and Ψ^{LR} the Kohn-Sham determinant, when the coupling parameter μ of Eq. (1) approaches zero. Thus, Ψ^{LR} is not the true wave function of the system: It does not explicitly contain short-range exchange-correlation effects, and approaches the true wave function of the system only in the limit $\mu\to\infty$. Note also that the computational effort of the mixed method equals the effort of the corresponding *ab initio* method plus an additional DFT calculation. In the following it will be shown why this method nevertheless offers interesting features.

With an exact $E_{\mathrm{xc}}^{\mathrm{SR}}$ (and in the limit of an exact long-range wave function), the results should be independent of the coupling parameter μ in Eq. (1). For the following calculations we chose $\mu=0.5$, which was found to be a reasonable compromise between accuracy and efficiency (cf. [23,26]).

The key point in the CAM DFT approximation is a more general split of the Coulomb operator, compared to Eq. (1),

$$V_{ee} = \sum_{i<j}\frac{1-[\alpha+\beta\operatorname{erf}(\mu r_{ij})]}{r_{ij}} + \sum_{i<j}\frac{\alpha+\beta\operatorname{erf}(\mu r_{ij})}{r_{ij}}, \tag{10}$$

where the two parameters α and β have to satisfy the constraints $0\leqslant\alpha+\beta\leqslant 1$, $0\leqslant\alpha\leqslant 1$, and $0\leqslant\beta\leqslant 1$. The parameter α determines the weight of the Hartree-Fock (HF) exchange for all distances, while additional long-range HF exchange is mixed in with parameter β. As DFT part we used the B3LYP functional [14]—the Coulomb-attenuated form therefore is called CAM B3LYP [16], with $\alpha=0.19$, $\beta=0.46$, and $\mu=0.33$. The original routines have been written by Salek [17] and recently implemented into the program package DIRAC [27].

TABLE I. Dipole moments μ_D (D) of CuX, AgX, and AuX (X=H, F, Cl, Br, and I) from standard HF calculations and from DFT calculations using the LDA, PBE, B3LYP, and CAM B3LYP functionals, with basis set A (see text), and from basis set extrapolated standard CCSD(T) calculations (CBS). Experimental data (Expt.) are taken from Refs. [40,43–45]; errors in the last digit are quoted in parentheses. Note that the first six columns have been calculated in all-electron four-component relativistic calculations. Nevertheless, we compare these values with the scalar-relativistic results in the last column, because the spin-orbit correction is small. The contribution of the latter is evaluated at the CAM B3LYP level, where spin-free results are given in the SF CAM B3LYP column.

	Basis A						CBS [45]	
	LDA	PBE	B3LYP	CAM B3LYP	SF CAM B3LYP	HF	CCSD(T)	Expt.
CuH	1.92	2.07	2.38	2.63	2.63	3.88	2.71	
CuF	4.39	4.40	4.87	5.11	5.11	6.13	5.29	5.77(20) [43]
CuCl	4.10	4.19	4.63	4.94	4.95	6.19	5.19	
CuBr	3.82	3.92	4.40	4.77	4.78	6.24	4.94	
CuI	3.32	3.46	3.94	4.38	4.47	6.06	4.60	
AgH	2.17	2.40	2.68	2.98	2.98	4.10	2.92	
AgF	5.08	5.13	5.59	5.86	5.87	6.81	6.04	6.22(20) [43]
AgCl	4.80	4.99	5.38	5.76	5.77	6.92	5.95	6.076(60) [44]
AgBr	4.49	4.69	5.12	5.58	5.59	6.97	5.67	5.620(30) [45]
AgI	3.91	4.16	4.57	5.12	5.22	6.73	5.27	4.550(50) [40]
AuH	0.88	1.04	1.24	1.47	1.49	2.45	1.37	
AuF	3.44	3.45	3.91	4.24	4.31	5.40	4.37	
AuCl	2.86	3.00	3.38	3.79	3.86	5.14	3.90	
AuBr	2.46	2.61	2.99	3.44	3.48	4.99	3.48	
AuI	1.86	2.06	2.41	2.89	2.98	4.61	2.94	
MAD	1.01	0.87	0.48	0.13	0.11	1.20		
D	−1.01	−0.87	−0.48	−0.11	−0.08	1.20		
$\sigma(\Delta)$	0.21	0.21	0.14	0.10	0.10	0.25		

III. COMPUTATIONAL DETAILS

The experimental bond distances of the group-11 hydrides and halides are taken from Ref. [28] for the Cu and Ag compounds and for AuH, and from Refs. [29–31] for the Au halides. As the first-order density matrix is not available for MP2 and CCSD, dipole moments μ_D were determined by calculating the energy E for different electric field strengths F ($F_1=-2\Delta F$, $F_2=-\Delta F$, $F_3=\Delta F$, $F_4=2\Delta F$, $\Delta F=0.001$ a.u.) and using numerical differentation:

$$\mu_D = \left| \frac{E(F_1) - 8E(F_2) + 8E(F_3) - E(F_4)}{12\Delta F} \right|. \tag{11}$$

Note that the LDA, PBE, B3LYP, and CAM B3LYP as well as the HF calculations of Table I were all-electron four-component relativistic calculations carried out using the program DIRAC [27], based on the Dirac-Coulomb Hamiltonian. We used our own optimized basis sets with ($20s16p11d3f$) for Cu, ($21s22p12d4f$) for Ag, and ($26s24p16d12f$) for Au. For the halides we used the following basis sets: ($13s7p4d$) for F, ($17s12p4d$) for Cl, ($19s17p9d2f$) for Br, and ($20s19p11d2f$) for I. The basis set for hydrogen was ($11s6p4d3f$). This basis will be referred to as basis A in the following. In order to study the influence of spin-orbit effects and to be able to directly compare to the scalar-relativistic pseudopotential results we also performed spin-free (SF) CAM B3LYP calculations.

All SR DFT–LR *ab initio* calculations [DFT=LDA, PBE; *ab initio*=HF, MP2, CCSD, CCSD(T)] of Table II were performed employing our recent implementation in the MOLPRO 2006 *ab initio* suite of programs [32]. In these calculations, we applied augmented correlation consistent polarized valence triple-ζ (aug-cc-pVTZ) basis sets for hydrogen, fluorine [33,34], and chlorine [35]. Energy-consistent relativistic effective core potentials [36,37] were used together with aug-cc-pVTZ valence basis sets for bromine and iodine [36], and with cc-pVTZ valence basis sets for the metal atoms [38]. This basis will be denoted as basis B in the following.

As accurate experimental dipole moments for the group-11 halides are scarce, we determined high-accuracy reference values. They were calculated from the (aug-)cc-pV5Z HF energies and from extrapolations of the (aug-)cc-pVnZ ($n=4,5$) correlation energies to the complete basis set limit (CBS) according to $E_c = E_{CBS} + an^{-3}$ [39].

TABLE II. Dipole moments μ_D (D) of CuX, AgX, and AuX, (X=H, F, Cl, Br, and I) from DFT calculations, from *ab initio* HF, MP2, CCSD, and CCSD(T) calculations, and from the corresponding mixed SR DFT–LR *ab initio* calculations, with basis set B (see text). In each column with DFT values two adjacent numbers are given, which refer to LDA and PBE results, respectively. Comparison is made to basis set extrapolated standard CCSD(T) calculations (CBS). For experimental results, see Table I.

	Basis B														CBS
	DFT		DFT-HF		DFT-MP2		DFT-CCSD		DFT-CCSD(T)		HF	MP2	CCSD	CCSD(T)	CCSD(T)
CuH	1.98	2.17	3.15	3.20	2.94	2.99	2.81	2.86	2.80	2.85	3.95	2.95	3.07	2.87	2.71
CuF	4.43	4.44	5.57	5.55	5.41	5.40	5.32	5.30	5.31	5.28	6.20	5.41	5.60	5.43	5.29
CuCl	4.17	4.31	5.55	5.56	5.30	5.31	5.20	5.21	5.17	5.18	6.26	5.30	5.51	5.30	5.19
CuBr	3.80	3.96	5.33	5.35	5.01	5.03	4.91	4.93	4.87	4.89	6.17	5.07	5.29	5.06	4.94
CuI	3.41	3.59	5.10	5.12	4.71	4.74	4.60	4.63	4.56	4.59	6.00	4.74	4.98	4.71	4.60
AgH	2.14	2.38	3.45	3.53	3.10	3.18	2.99	3.06	2.97	3.04	4.17	3.15	3.24	3.08	2.92
AgF	5.06	5.14	6.33	6.32	6.13	6.12	6.04	6.03	6.02	6.01	6.90	6.28	6.35	6.19	6.04
AgCl	4.74	4.95	6.33	6.36	5.98	6.02	5.88	5.91	5.85	5.88	6.99	6.15	6.24	6.06	5.95
AgBr	4.33	4.56	6.08	6.12	5.65	5.70	5.54	5.59	5.50	5.55	6.88	5.86	5.97	5.77	5.67
AgI	3.88	4.13	5.82	5.87	5.28	5.34	5.18	5.24	5.13	5.18	6.69	5.44	5.59	5.36	5.27
AuH	0.94	1.12	1.92	2.00	1.54	1.61	1.49	1.57	1.48	1.55	2.53	1.30	1.59	1.45	1.37
AuF	3.58	3.62	4.91	4.91	4.59	4.59	4.47	4.46	4.44	4.43	5.51	4.57	4.70	4.46	4.37
AuCl	2.97	3.15	4.54	4.59	4.02	4.08	3.93	3.99	3.89	3.94	5.25	3.98	4.17	3.94	3.90
AuBr	2.48	2.69	4.16	4.23	3.54	3.61	3.47	3.54	3.42	3.49	5.04	3.51	3.76	3.52	3.48
AuI	1.97	2.20	3.75	3.83	3.02	3.11	2.97	3.06	2.92	3.01	4.72	2.87	3.22	2.96	2.94
MAD	0.98	0.81	0.49	0.53	0.11	0.15	0.06	0.07	0.07	0.07	1.24	0.15	0.31	0.10	
D	−0.98	−0.81	0.49	0.53	0.11	0.15	0.01	0.05	−0.02	0.02	1.24	0.13	0.31	0.10	
$\sigma(\Delta)$	0.24	0.23	0.14	0.17	0.07	0.08	0.07	0.08	0.08	0.08	0.23	0.10	0.04	0.04	

These values are supposed to be quite accurate and mostly agree fairly well with the experimental values. However, we found a deviation of over 0.7 D in the case of the AgI molecule, where we calculated 5.27 D compared to the experimental value of about 4.55 D [40]. Using the continued-fraction formalism of Goodson [41] we approximated the full configuration-interaction limit from HF, CCSD, and CCSD(T) data, and found that the correction due to higher-order excitations does not exceed 0.03 D for AgI. Comparing CAM B3LYP and SF CAM B3LYP reveals that spin-orbit corrections are about 0.1 D (cf. Table I); core-valence correlation also seems to play a certain role: Treating the outer core $4s4p$ shell of Ag at the correlated level further diminishes the difference by roughly 0.15 D. All these effects cannot fully account for the observed difference between basis set extrapolated CCSD(T) and experiment, but we note that an earlier measurement of Hoeft and Nair (5.10 D) [42] agrees much better with our theoretical findings.

For all data sets we calculated the mean absolute deviation (MAD) with respect to the complete basis set extrapolated CCSD(T) values μ_D^{ref}, the mean deviations (D), and the standard deviation of the errors [$\sigma(\Delta)$], where

$$\sigma(\Delta) = \sqrt{\sum_{i=1}^{N} \frac{[(\mu_{D_i} - \mu_{D_i}^{\mathrm{ref}}) - D]^2}{N}}. \qquad (12)$$

IV. RESULTS AND DISCUSSION

The question is whether or not sensitive properties like dipole moments undergo a substantial improvement when mixing short-range density-functional-based with long-range wave-function-based methods. Tables I and II contain the results of our calculations at the CAM B3LYP (Table I) and SR DFT–LR CC (Table II) levels of theory. Clearly, we observe what has been pointed out before [5,6], i.e., the functionals currently in use in DFT approximations not only yield dipole moments with rather large MADs of 0.4 to 1.0 D, they also scatter substantially with $\sigma(\Delta)$ of up to 0.24 D. This is illustrated in Figs. 1 and 2.

We note that the CAM B3LYP approximation, differently from its borderline cases B3LYP and HF, yields quite good results already: whereas B3LYP with a MAD of 0.48 and $\sigma(\Delta)$ of 0.14 clearly underestimates the dipole moments of group-11 hydrides and halides, and HF with a MAD of 1.20 and $\sigma(\Delta)$ of 0.25 drastically overestimates them, CAM B3LYP only slightly overestimates them with a MAD of 0.13 and $\sigma(\Delta)$ of 0.10. A comparison with the spin-free calculations (SF CAM B3LYP) shows that spin-orbit effects are rather small (<0.1 D), as they are only of second order. Four-component LDA and PBE results are also included in Table I, which can be compared to the corresponding scalar relativistic pseudopotential results in Table II. Differences between both results are mainly due to inclusion of spin-orbit coupling and the different basis sets used.

We now compare our best results—namely, SR PBE–LR CCSD(T) ones—with the pure PBE and pure CCSD(T) limit: SR PBE–LR CCSD(T) yields maximum errors of 0.18 D overestimation (AuH) and of 0.12 D underestimation (AgBr) for the hydrides and halides, respectively. The mean

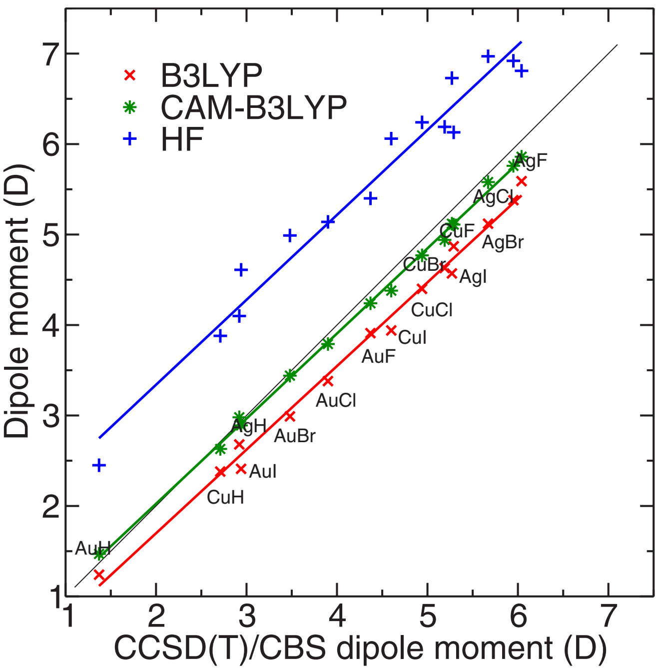

FIG. 1. (Color online) Calculated dipole moments μ_D (D) of CuX, AgX, and AuX (X=H, F, Cl, Br, and I) versus the CCSD(T) basis set limit values. Calculations were performed using pure B3LYP, CAM B3LYP, and pure HF with basis A.

absolute deviation is 0.07 D, $\sigma(\Delta)$ 0.08 D. The maximum error of the PBE functional is an underestimation of 0.54 D (CuH, AgH) and of 1.14 D (AgI) for the hydrides and halides, respectively. The MAD amounts to 0.81 D, $\sigma(\Delta)$ is 0.23 D. Thus, the PBE results can be improved by an order of magnitude when mixing in LR CCSD(T). The scattering behavior also becomes better: $\sigma(\Delta)$ decreases to one-third of its original value for the mixed calculation. The CCSD(T) maximum errors are much better than the PBE ones: We find an overestimation of 0.16 D (CuH, AgH) and of 0.15 D (AgF) for the hydrides and halides, respectively. The CCSD(T) MAD is a bit larger than for the mixed method, namely, 0.1 D, whereas its $\sigma(\Delta)$ is somewhat smaller–half as big as for the mixed method. The SR PRB–LR CCSD(T) results are thus comparable to pure CCSD(T) results.

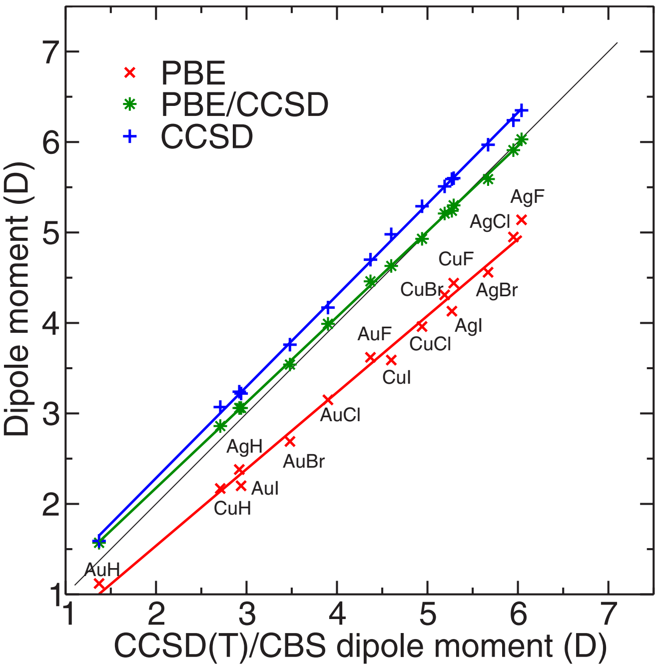

FIG. 2. (Color online) Calculated dipole moments μ_D (D) of CuX, AgX, and AuX (X=H, F, Cl, Br, and I) versus the CCSD(T) basis set limit values. Calculations were performed using pure PBE, the SR PBE–LR CCSD method, and pure CCSD with basis B.

Let us now study how the modification of the DFT level affects the results: Using pure LDA instead of pure PBE leads to a MAD deterioration of about 0.2 D, whereas the standard deviation of the error increases only by 0.01 D. In contrast, using SR LDA instead of SR PBE leaves the MAD and $\sigma(\Delta)$ unchanged, and only the mean deviation (D) undergoes a small change from 0.02 D to -0.02 D. Not only can the LDA results be ameliorated by an order of magnitude by mixing in LR CCSD(T)—the outcomes are even nearly indistinguishable from SR PBE–LR CCSD(T) results. The situation changes for DFT functionals with full exact exchange, denoted as DFT(c). LDA(c) as well as PBE(c) overestimate the dipole moment by over 1.3 D, $\sigma(\Delta)$ is about 0.25 D; admixture of LR CCSD(T) only slightly reduces the MAD to roughly 1.0 D and halves $\sigma(\Delta)$. Once more it turns out that the combination of nonlocal HF exchange with local DFT correlation is less recommendable than DFT with a local description of both exchange and correlation.

Altering the theoretical level on the *ab initio* side from CCSD(T) to CCSD significantly deteriorates the MAD from 0.1 to 0.31 D. The SR PBE–LR CCSD MAD, however, is exactly the same as the SR PBE–LR CCSD(T) MAD; only the D changes by 0.03 D; $\sigma(\Delta)$ is unaffected for CCSD and SR PBE–LR CCSD, respectively. Basically the same happens when using SR LDA LR CCSD. This means that for the mixed method, triples can be omitted without any loss of quality, in contrast to the pure *ab initio* case. This is in line with our previous findings [22,23]. Note that dipole moments calculated with pure MP2 have a MAD of not more than 0.15 D and a $\sigma(\Delta)$ of 0.1 D, outperforming the pure CCSD results. Mixing in of SR DFT leaves these more or less unmodified.

Comparing the pure LDA and pure HF limits with the SR LDA–LR HF method (Table II) reveals the role of LR correlation: Though the mixture of both methods approximately halves the MAD from 0.98 D in LDA and 1.24 D in HF to 0.49 D in SR LDA–LR HF and diminishes $\sigma(\Delta)$ from 0.24 D in LDA and 0.23 D in HF to 0.14 D in SR LDA–LR HF, the correlation contribution that is required to reach the SR DFT–LR CCSD (T) values of 0.07 D MAD and 0.08 D $\sigma(\Delta)$ is considerable.

Unfortunately, the basis set dependency of the mixed methods is not better (rather slightly worse) than for the pure *ab initio* method. This was shown by appropriately extending our calculations from a basis of triple-ζ quality (basis B) to a basis of quadruple-ζ quality. Presumably, this is due to the fact that the pure DFT methods also show an unexpectedly large basis set dependency, which also seems to affect the basis set dependency of the mixed methods. Nevertheless, the results for the mixed methods with quadruple-ζ basis are still very satisfying: SR PBE–LR CCSD(T), for example, has a MAD of 0.09 D and a $\sigma(\Delta)$ of 0.09 D.

V. CONCLUSIONS

The CAM B3LYP approximation describes dipole moments of all group-11 hydrides and halides reasonably well, and we hope that this method could also be applied for the calculation of electric properties in other transition-metal-containing compounds. The mixture of SR DFT (LDA or PBE with local DFT exchange) and LR CCSD further improves the situation and yields excellent results already for a medium size basis of triple-ζ quality. They show a smaller MAD than the CCSD(T) results with the same basis set quality though the computational cost for the mixed method is lower. To get results that surpass SR DFT–LR CCSD calculations with triple-ζ basis sets, at least CCSD(T) calculations with quadruple-ζ basis sets are required. Interestingly, in the case of the mixed methods, the effect of perturbative triples is nearly negligible. The mixed method seems to be less sensitive to both the quality of the density functionals and the level of *ab initio* correlation treatment than pure DFT or *ab initio* methods.

ACKNOWLEDGMENTS

Financial support from the Deutsche Forschungsgemeinschaft in Germany (Priority Program SPP1145), Marsden Grant (No. 06-MAU-057), and the ISAT Linkage Fund in New Zealand is gratefully acknowledged. We are grateful to Pawel Salek (Stockholm) and Trond Saue (Strasbourg) for CAM B3LYP routines.

[1] W. Kohn, Y. Meir, and D. E. Makarov, Phys. Rev. Lett. **80**, 4153 (1998).

[2] N. Kurita and H. Sekino, Int. J. Quantum Chem. **91**, 355 (2001).

[3] M. Cococcioni and S. de Gironcoli, Phys. Rev. B **71**, 035105 (2005).

[4] V. I. Anisimov, J. Zaanen, and O. K. Andersen, Phys. Rev. B **44**, 943 (1991).

[5] P. Schwerdtfeger, M. Pernpointer, and J. K. Laerdahl, J. Chem. Phys. **111**, 3357 (1999).

[6] E. van Lenthe and E. J. Baerends, J. Chem. Phys. **112**, 8279 (2000).

[7] J. N. Harvey, in *Structure and Bonding*, edited by N. Kaltsoyannis and J. E. McGrady (Springer, Heidelberg, 2004), pp. 151–184.

[8] A. Hermann, B. Vest, and P. Schwerdtfeger, Phys. Rev. B **74**, 224402 (2006).

[9] H. Stoll and A. Savin, in *Density Functional Methods in Physics*, edited by R. Dreizler and J. da Providencia (Plenum, New York, 1985), pp. 177–207.

[10] A. Savin and H.-J. Flad, Int. J. Quantum Chem. **56**, 327 (1995).

[11] T. Leininger, H. Stoll, H.-J. Werner, and A. Savin, Chem. Phys. Lett. **275**, 151 (1997).

[12] J. Toulouse, F. Colonna, and A. Savin, Phys. Rev. A **70**, 062505 (2004).

[13] T. Söhnel, H. Hermann, and P. Schwerdtfeger, J. Phys. Chem. B **109**, 526 (2005).

[14] A. D. Becke, J. Comput. Chem. **20**, 63 (1999).

[15] R. Bast and P. Schwerdtfeger, J. Chem. Phys. **119**, 5988 (2003).

[16] T. Yanai, D. P. Tew, and N. C. Handy, Chem. Phys. Lett. **393**, 51 (2004).

[17] M. J. G. Peach, T. Helgaker, P. Salek, T. W. Keal, O. B. Lutnæs, D. J. Tozer, and N. C. Handy, Phys. Chem. Chem. Phys. **8**, 558 (2006).

[18] C. Hampel, K. Peterson, and H.-J. Werner, Chem. Phys. Lett. **190**, 1 (1992).

[19] M. J. O. Deegan and P. J. Knowles, Chem. Phys. Lett. **227**, 321 (1994).

[20] A. Savin, in *Recent Developments and Applications of Modern Density Functional Theory*, edited by J. M. Seminario (Elsevier, Amsterdam, 1996), pp. 327–357.

[21] S. Paziani, S. Moroni, P. Gori-Giorgi, and G. B. Bachelet, Phys. Rev. B **73**, 155111 (2006).

[22] E. Goll, H.-J. Werner, and H. Stoll, Phys. Chem. Chem. Phys. **7**, 3917 (2005).

[23] E. Goll, H.-J. Werner, H. Stoll, T. Leininger, P. Gori-Giorgi, and A. Savin, Chem. Phys. **329**, 276 (2006).

[24] J. P. Perdew, K. Burke, and M. Ernzerhof, Phys. Rev. Lett. **77**, 3865 (1996).

[25] M. Levy, Proc. Natl. Acad. Sci. U.S.A. **76**, 6062 (1979).

[26] I. C. Gerber and J. G. Ángyán, Chem. Phys. Lett. **415**, 100 (2005).

[27] H. J. A. Jensen *et al.*, computer code DIRAC, Release 04.0 (2004), URL http://dirac.chem.sdu.dk

[28] K. P. Huber and G. Herzberg, *Molecular Spectra and Molecular Structure: Constants of Diatomic Molecules* (Van Nostrand, New York, 1979).

[29] C. J. Evans and M. C. L. Gerry, J. Mol. Spectrosc. **203**, 105 (2000).

[30] C. J. Evans and M. C. L. Gerry, J. Am. Chem. Soc. **122**, 1560 (2000).

[31] L. M. Reynolds, C. J. Evans, and M. C. L. Gerry, J. Mol. Spectrosc. **205**, 344 (2001).

[32] R. D. Amos *et al.*, computer code MOLPRO, version 2006.2 (2006), URL http://www.molpro.net/

[33] T. H. Dunning, Jr., J. Chem. Phys. **90**, 1007 (1989).

[34] R. Kendall, T. H. Dunning, Jr., and R. Harrison, J. Chem. Phys. **96**, 6796 (1992).

[35] D. Woon and T. H. Dunning, Jr., J. Chem. Phys. **98**, 1358 (1993).

[36] K. A. Peterson, D. Figgen, E. Goll, H. Stoll, and M. Dolg, J. Chem. Phys. **119**, 11113 (2003).

[37] D. Figgen, G. Rauhut, M. Dolg, and H. Stoll, Chem. Phys. **311**, 227 (2005).

[38] K. A. Peterson and C. Puzzarini, Theor. Chem. Acc. **114**, 283 (2005).
[39] T. Helgaker, W. Klopper, H. Koch, and J. Noga, J. Chem. Phys. **106**, 9639 (1997).
[40] K. P. R. Nair and J. Hoeft, Phys. Rev. A **29**, 1889 (1984).
[41] D. Z. Goodson, J. Chem. Phys. **116**, 6948 (2002).
[42] J. Hoeft and K. P. R. Nair, J. Mol. Struct. **97**, 347 (1983).
[43] J. Hoeft, F. J. Lovas, E. Tiemann, and T. Törring, Z. Naturforsch. A **25**, 35 (1970).
[44] K. P. R. Nair and J. Hoeft, J. Phys. B **17**, 735 (1984).
[45] K. P. R. Nair and J. Hoeft, Chem. Phys. Lett. **102**, 438 (1983).